

POLITECNICO DI TORINO  
Repository ISTITUZIONALE

A spread spectrum clock generator based on a short-term optimized chaotic map

*Original*

A spread spectrum clock generator based on a short-term optimized chaotic map / Pareschi, F.; Setti, G.; Rovatti, R.; Frattini, G.. - STAMPA. - (2011), pp. 507-510. (Intervento presentato al convegno 37th European Solid-State Circuits Conference, ESSCIRC 2011 tenutosi a Helsinki, fin nel September 12-16, 2011) [10.1109/ESSCIRC.2011.6044933].

*Availability:*

This version is available at: 11583/2850208 since: 2020-10-28T10:09:07Z

*Publisher:*

IEEE Computer Society

*Published*

DOI:10.1109/ESSCIRC.2011.6044933

*Terms of use:*

This article is made available under terms and conditions as specified in the corresponding bibliographic description in the repository

*Publisher copyright*

IEEE postprint/Author's Accepted Manuscript

©2011 IEEE. Personal use of this material is permitted. Permission from IEEE must be obtained for all other uses, in any current or future media, including reprinting/republishing this material for advertising or promotional purposes, creating new collecting works, for resale or lists, or reuse of any copyrighted component of this work in other works.

(Article begins on next page)

# A Spread Spectrum Clock Generator Based on a Short-term Optimized Chaotic Map

Fabio Pareschi<sup>\*†</sup>, Gianluca Setti<sup>\*†</sup>, Riccardo Rovatti<sup>†‡</sup> and Giovanni Frattini<sup>§</sup>

<sup>\*</sup>ENDIF – Engineering Department, University of Ferrara. Via Saragat, 1 – 44122 Ferrara, Italy

<sup>†</sup>DEIS – Department of Electronics, Computer Sciences and Systems, University of Bologna.

Viale Risorgimento, 2 – 40136 Bologna

<sup>‡</sup>Research Center “ARCES” – University of Bologna. Via Toffano, 2 – 40125 Bologna

<sup>§</sup>National Semiconductor, Italy.

Email: {fabio.pareschi, gianluca.setti}@unife.it,  
riccardo.rovatti@unibo.it, giovanni.frattini@nsc.com

**Abstract**—We present a spread spectrum clock generator for EMI reduction, where the modulating signal is generated by a suitably designed chaotic map. With respect to past solutions, the map has been designed to achieve a specific short-term behavior of the generated sequences, which allows to optimize the electromagnetic interference peak reduction not only for the theoretical spectrum, but also in the measurement setting prescribed by CISPR norms. In the latter case, we are able to achieve a 3.8 dB improvement in EMI reduction with respect to the triangular modulation when using the peak detector, which increases to 6.9 dB when switching to the quasi-peak detector. Results are measured on a prototype which has been designed and fabricated in a 0.18  $\mu\text{m}$  CMOS technology.

## I. INTRODUCTION

The Electro-Magnetic Interferences (EMI) reduction in clocked signals in integrated digital or mixed-signal circuits is of great practical concern. In particular, *design-time* solutions have to be adopted [1] whenever *a-posteriori* methodologies, such filtering or shielding methodologies cannot be employed, since they may very likely not ensure the required reduction, or simply since they may be not economically convenient. The basic idea in the former solutions is to introduce in the reference clock an intentional *jitter* by slightly *delaying* or *anticipating* clock edges, thus avoiding perfect periodicity and reshaping the power spectrum from a delta-like function to a wide-band spectrum so reducing the power spectrum peak level. This point of view is perfectly coherent with international regulations [2], [3], which link compliance with the ability of fitting the interfering power spectrum within a prescribed mask.

The most common way to spread the spectrum of timing signal (and therefore of all voltages/currents synchronous to it) is to frequency modulate the clock itself using a triangular waveform as driving signal. This solution represents a very good trade-off between performances and hardware complexity, and it is widely employed. For example, it is adopted by the Serial-ATA protocol to mitigate EMI related problems [4], [5], [6], [7]. On the other hand, better results can be achieved by using suitably designed periodic driving signals [1] or aperiodic signals, in particular chaos-based ones [8], where the driving signal is generated by means of a 1-D discrete time chaotic system also known as *chaotic map* [9]. More specifically, chaotic modulations has been shown to achieve the best results in terms of the peak value of the EMI theoretical spectrum, thanks to the fact that it is possible to achieve a complete flat power spectrum without any discrete component, which represents the optimum in terms of EMI reduction. A sketch comparison between the two approaches can be observed in Figure 1.

In this paper we present a Spread-Spectrum Clock Generator (SSCG) where the spreading of the spectrum is achieved by

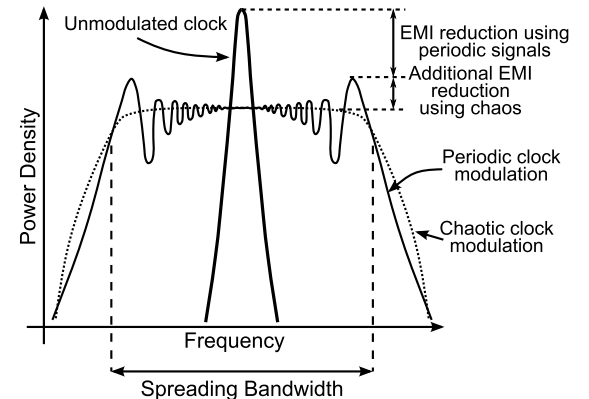


Figure 1. Comparison between the power spectra of an unmodulated clock (bold line), a periodic-modulated clock (dotted line) and of a chaotic-modulated clock (solid line). As any periodic modulation presents a power spectrum with some ringing effect, it is outperformed in EMI reduction by the non-periodic chaotic modulation.

means of a chaotic map. The difference with respect to solutions already proposed in the literature [10], [11] is that the chaotic map presented here does not only optimize the EMI reduction from the point of view of the theoretical spectrum, but it also takes into account the model of the EMI receiver and optimizes the power spectrum measured with the latter. The input/output behavior of an EMI receiver [12] is far from trivial and, if one takes it into account, specific setting exists in which the measured spectrum can be even far from the theoretical one, so that ensuring the optimal EMI reduction in terms of theoretical spectrum may not guarantee to achieve the minimum interference when measured according to EMI regulations. Experimental results on a prototype implemented in 0.18  $\mu\text{m}$  CMOS technology and designed following this approach show that we can achieve a 3.8 dB advantage with respect to the triangular modulation using the peak detector on a HP 8546 EMI receiver, and 6.9 dB advantage when using the quasi-peak detector.

The paper is organized as follows. In Section II we present a brief model of the EMI receiver, upon which we are able to extract which features a driving signal must have in order to ensure a low measured interference spectrum level. In the same section we also present a chaotic circuit for generating a driving signal capable of achieving both the optimum theoretical power spectrum and very good performances in terms of measured spectrum. In Section III we present a brief description of the fabricated prototype, while in IV we show the measurement results. Section V reports the

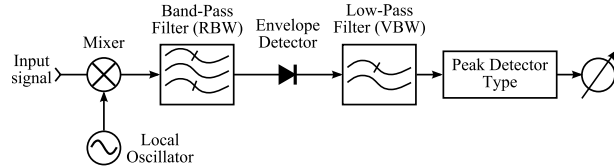


Figure 2. Block diagram of an analog Spectrum Analyzer.

conclusion.

## II. OPTIMIZATION OF THE MEASURED SPECTRUM

### A. EMI Receiver Model

An EMI receiver is basically an analog Spectrum Analyzer, and works as the superheterodyne receiver schematized in Figure 2 [12]. The input signal is mixed with a pure tone generated by a local oscillator to shift it in frequency and then filtered by narrow band-pass filter, whose bandwidth is so-called Resolution BandWidth (RBW). The resulting output signal is then demodulated by an envelope detector, put at the input of a low-pass filter of bandwidth VBW, whose output power level is measured by a peak detector. By changing the local oscillator frequency, it is possible to tune a different frequency and to get a measure of all the signal power spectrum.

The EMI regulations allows the use of both the *quasi-peak detector* and the *positive peak detector*. The behavior of the two detectors is similar and quite complex. While a full description is out of the purpose of this paper, it is here enough to recall that the quasi-peak detector attenuates the effect of erratic peaks in the signal power and that, when the input signal is a single tone (or it is composed by components whose distance is much greater than RBW), both detectors indicate the exact signal power, while conversely, the power is overestimated.

In particular, under the assumption of a frequency modulation of a single tone or of a periodic signal (like a clock), i.e. when we can describe the input signal as changing its instantaneous frequency in time, it is very simple to see from the instrument mathematical model that the longer the time in which the instantaneous frequency continuously stays (also considering the translation effect of the mixer) in the bandwidth of the RBW filter, the higher the overestimation. In this case, the input signal appears almost unmodulated to the instrument, which erroneously estimate the power up to a value as large as the total power of the input signal. On the contrary, the fastest the instantaneous frequency exits from the RBW filter bandwidth, the more similar the estimated power to the theoretical one.

### B. Chaotic Map Design

Chaotic maps [9] are 1D discrete-time autonomous systems, whose evolution is described by:

$$x_{k+1} = M(x_k), \quad M : I \mapsto I \quad (1)$$

where  $M$  is a non-linear function that maps an interval  $I$  into itself. The main property of these systems is the strong dependence on the initial condition: two trajectories starting from two very close initial conditions appear, after few steps, as completely uncorrelated. This guarantees unpredictability in true-implemented systems, where the system state  $x_k$  is known only with finite precision. However the property which make these system suitable for EMI reduction is to generate non periodic trajectories, which ensure a *continuous* power spectrum of the clock frequency modulated by it. Note that the above properties require an intrinsically analog implementation; any finite precision implementation, i.e. any *digital* approximation of (1), will result in a finite-state machine, which always achieves a periodic behavior.

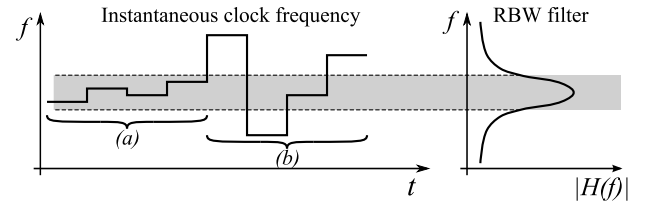


Figure 3. Basic explanation of the short-term effect on the peak detector. When the signal instantaneous frequency is almost unchanged for few subsequent time steps as in (a), the EMI receiver overestimates its power; in (b) the measured power is almost correct.

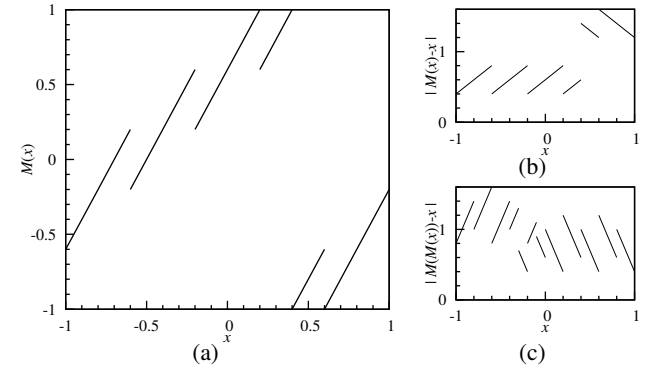


Figure 4. (a)  $M$  function of the chaotic map used in the presented prototype, normalized into the interval  $I = [-1, 1]$ . This map has been designed to get  $|M(x) - x| > 0.4$  (plot (b)) and  $|M(M(x)) - x| > 0.4$  (plot (c)).

By using advanced mathematical tools to analyze these systems [9], one can prove that by properly designing the  $M$  function is possible to control the statistical properties of the sequence  $x_k$ . In particular it is very easy to achieve a desired first order statistics, i.e. the probability density  $\rho(x_k)$  of the symbols  $x_k$  such that  $\Pr\{y \leq x_k \leq y + dy\} = \rho(y)dy$ .

In [10] it is extensively discussed the idea to replace the triangular driving signal with the PAM signal

$$\xi(t) = \sum_k x_k g(t - kT_s) \quad (2)$$

where  $g(t)$  is a rectangular pulse of duration  $T_s$ , and the sequence  $\{x_k\}$  comes from a chaotic map. The advantage is to achieve a continuous power spectrum whose shape is exactly the symbol density  $\rho(x_k)$ . Hence, if  $\rho(x_k)$  is uniform, the theoretical spectrum is completely flat in the spreading bandwidth, which results in the optimal condition for EMI reduction.

The main contribution of this paper is to take into account the EMI receiver model to add some constraints on the design of the optimal  $M$  function. If one wishes to minimize the EMI measured in this setting, overestimation of the spectrum must be avoided, which requires that, accordingly to what has been noted in Section II-A, the instantaneous frequency of the modulated clock *a*) needs to be varied rapidly, and *b*) must be modified to a value which is never too close to the previous one. This is explained in Figure 3, and requires that, in the chaotic PAM signal *a*)  $T_s$  has to be short; and *b*) the short-term behavior has to be controlled in such way that the difference between contiguous symbols is large.

A chaotic map with the requested properties has been investigated, arriving to the solution reported in Figure 4-a. This map has an uniform  $\rho(x_k)$ , as required for optimizing the theoretical power spectrum, and also possess the desired short-term behavior, since there is a lower bound both on the difference

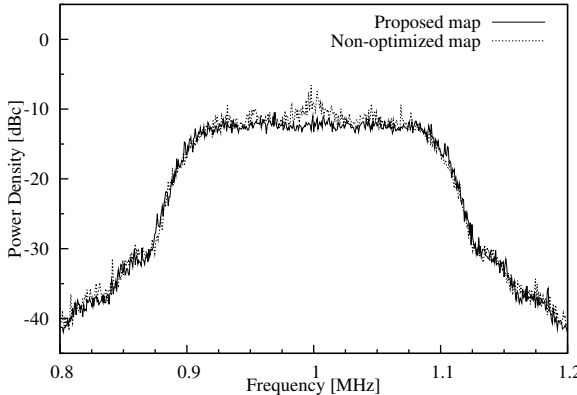


Figure 5. Comparison between the power spectrum of a chaotic modulation employing a standard, non-optimized chaotic map (dashed line, the map implemented in [11] has been used) and the proposed optimized map (solid line), achieved with a Matlab Spectrum Analyzer simulator.

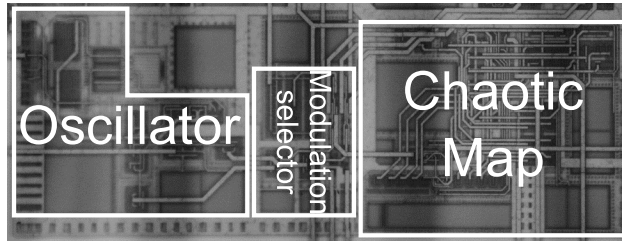


Figure 6. Microphotograph (detail) of the designed prototype.

$|x_{k+1} - x_k| = |M(x_k) - x_k|$  (Figure 4-b) and also on the difference  $|x_{k+2} - x_k| = |M(M(x_k)) - x_k|$  (Figure 4-c). The comparison between the spectrum achieved with an optimized and a non-optimized chaotic map (we used the map employed in [11] which, to the best of our knowledge, is the only other monolithic implementation of this technique, but with a completely different approach and for completely different applications) can be seen in Figure 5, where the shown spectra are achieved with a Matlab simulator of the Spectrum Analyzer. Despite the fact that both maps achieve the same optimized theoretical spectrum (the symbol density is the same) the difference in the above simulations is almost 5 dB.

### III. CIRCUIT IMPLEMENTATION

A prototype of a SSCG has been designed and fabricated in CMOS 0.18  $\mu\text{m}$  technology using thick oxide transistors (i.e. 5 V devices) only. The chip, whose microphotograph is shown in Figure 6, includes two instances of an oscillator capable of performing a frequency modulation and based on the charge/discharge of a capacitor with constant current. One of them is used to realize the triangular driving signal and the clock for the chaotic map; the other one for generating the spread spectrum clock. The oscillation frequency ranges from 0 to 2 MHz.

To keep a low complexity architecture, the chaotic map employs single-ended current signals, and its simplified block diagram is depicted in Figure 7. This circuit embeds both the sample/hold and the  $M$  function. The sample/hold ( $M_1$ - $M_4$ ) is closed into a loopback to achieve the update status function  $I_{k+1} = \alpha I_k$ . When  $I_k > I_{bp}^{(j)}$ , the pass transistor  $M_5$  turns on, and the update function is modified as  $I_{k+1} = \alpha I_k + I^{(j)}$ . By a proper design, and by replicating the circuit in the dashed box 5 times, the desired update function  $I_{k+1} = M(I_k)$  is achieved.

The total size of the chip active area is 360  $\mu\text{m} \times 270 \mu\text{m}$ , where

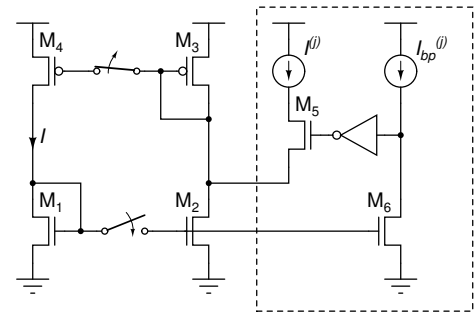


Figure 7. Block diagram of the chaotic map. The schematic is based on a current sample/hold which embeds the  $M$  function in the feedback path. The circuit in the dashed box adds a breakpoint at  $I_{bp}^{(j)}$  and is replicated 5 times with  $j = 1, 2, \dots, 5$  to generate the breakpoints of the  $M$  function.

140  $\mu\text{m} \times 120 \mu\text{m}$  are for the oscillators and 160  $\mu\text{m} \times 130 \mu\text{m}$  are for the chaotic map. The average current consumptions are 400  $\mu\text{A}$  and 250  $\mu\text{A}$  respectively, at a power supply voltage of 5 V.

### IV. MEASUREMENT RESULTS

To evaluate the performances of the chaotic map, we made a statistical analysis on the generated PAM signal, an example of which is shown in Figure 8. By plotting  $x_{k+1} vs x_k$  in long succession of map analog states  $\{x_k\}$  of the map one can reconstruct the actual  $M$  function implemented. Figure 9 shows the result of such a process, which is very close to the designed one.

Measurements on the modulated clock power spectrum have been obtained using an HP 8546A Spectrum Analyzer, which is certified for EMI measurements. Accordingly to CISPR regulations [3], we used the 9 kHz RBW EMI filter, and both the peak and the quasi-peak detector. Note that a comparison with existing works would not be fair, since measurements strongly depend on the measurement setup and on modulation parameters. The reason why we implemented the triangular modulation in the prototype is actually to fairly compare results with the state-of-the-art methodologies. For these measurements, the main oscillating frequency has been set to  $f_0 = 1 \text{ MHz}$ , with a spreading band equal to 0.9–1.1 MHz. Both a triangular modulation with a driving signal frequency  $f_m = 35 \text{ kHz}$  and a chaotic signal with  $1/T_s = 35 \text{ kHz}$  has been considered. The comparison is depicted in Figure 10 and shows that, when a peak detector is employed, the chaotic modulation outperforms the triangular one by 3.8 dB. Furthermore, when the measure is repeated in the neighborhood of the previously

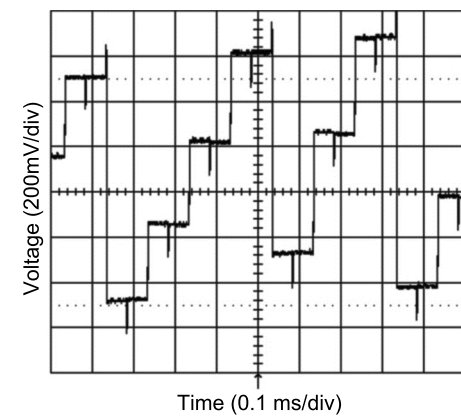


Figure 8. Example of the chaotic PAM signal.

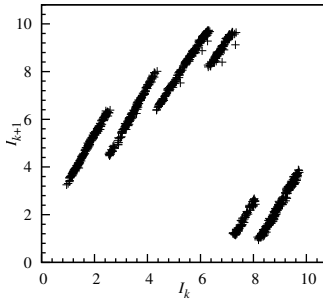


Figure 9.  $M$  function of the implemented chaotic map build with a scatter plot of a succession of measured analog states. Scales are in  $\mu\text{A}$ .

founded spectrum peaks and the quasi-peak detector is employed<sup>1</sup>, the difference grows to 6.9 dB.

## V. CONCLUSION

In this paper we have presented a prototype of a SSCG for EMI reduction based on the frequency modulation which employs a chaotic signal as driving signal. By considering a model of the EMI receiver, we were able to design a map which optimizes the theoretical power spectrum, and which also ensures that the measured spectrum is not overestimated. In this way we are able to obtain an advantage of 3.8 dB with respect to the classical triangular modulation when the peak detector is selected on the EMI receiver, and an advantage of 6.9 dB when the quasi-peak detector is selected.

<sup>1</sup>This is the standard approach in EMI measurements due to the long time required by the quasi-peak measurement and to the time constraints of the EMI receiver.

## REFERENCES

- [1] K. B. Hardin, J. T. Fessler, and D. R. Bush, "Spread spectrum clock generation for the reduction of radiated emissions," in *IEEE International Symposium on Electromagnetic Compatibility*, Aug. 1994, pp. 227–231.
- [2] Federal Communication Commission, "FCC methods of measurement of radio noise emission from computing devices," *FCC/OST MP-4*, 1987.
- [3] International Special Committee on Radio Interference (CISPR), Publication 16-1, 2004.
- [4] Y.-H. Kao and Y.-B. Hsieh, "A Low Power and High-Precision Spread Spectrum Clock Generator for Serial Advanced Technology Attachment applications Using Two-Point Modulation," *IEEE Transactions on Electromagnetic Compatibility*, vol. 51, no. 2, pp. 245–254, May 2009.
- [5] M. Kokubo *et al.*, "A Low-Jitter Spread Spectrum Clock Generator Using FDMP," *IEICE Trans. Elect.*, vol. E89-C, no. 11, Nov. 2006.
- [6] H.-R. Lee, O. Kim, G. Ahn, and D.-K. Jeong, "A low-jitter 5000ppm spread spectrum clock generator for multi-channel SATA transceiver in 0.18  $\mu\text{m}$  CMOS," in *IEEE International Solid-State Circuits Conference*, feb 2005, pp. 162–590.
- [7] D. Shen and S. Liu, "A Low-Jitter Spread Spectrum Clock Generator Using FDMP," *IEEE Transactions on Circuits and Systems II: Express Briefs*, vol. 54, no. 11, pp. 979–983, Nov. 2007.
- [8] G. Setti, M. Balestra, and R. Rovatti, "Experimental verification of enhanced electromagnetic compatibility in chaotic FM clock signals," in *IEEE Int. Symp. on Circuits and Systems*, May 2000, pp. 229–232.
- [9] A. Lasota and M. Mackey, *Chaos, Fractals, and Noise. Stochastic Aspects of Dynamics*, 2nd ed., ser. Applied Mathematical Sciences. Cambridge University Press, 1994, vol. 97.
- [10] S. Callegari, R. Rovatti, and G. Setti, "Spectral properties of chaos-based FM signals: theory and simulation results," *IEEE Transactions on Circuits and Systems I: Fundamental Theory and Applications*, vol. 50, no. 1, pp. 3–15, Jan. 2003.
- [11] F. Pareschi, G. Setti, and R. Rovatti, "A 3-GHz Serial ATA Spread-Spectrum Clock Generator Employing a Chaotic PAM Modulation," *IEEE Transactions on Circuits and Systems I: Regular Papers*, vol. 57, no. 10, pp. 2577–2587, Oct. 2010.
- [12] "Spectrum Analysis Basics," Agilent Application Note 150, Jun. 2006.

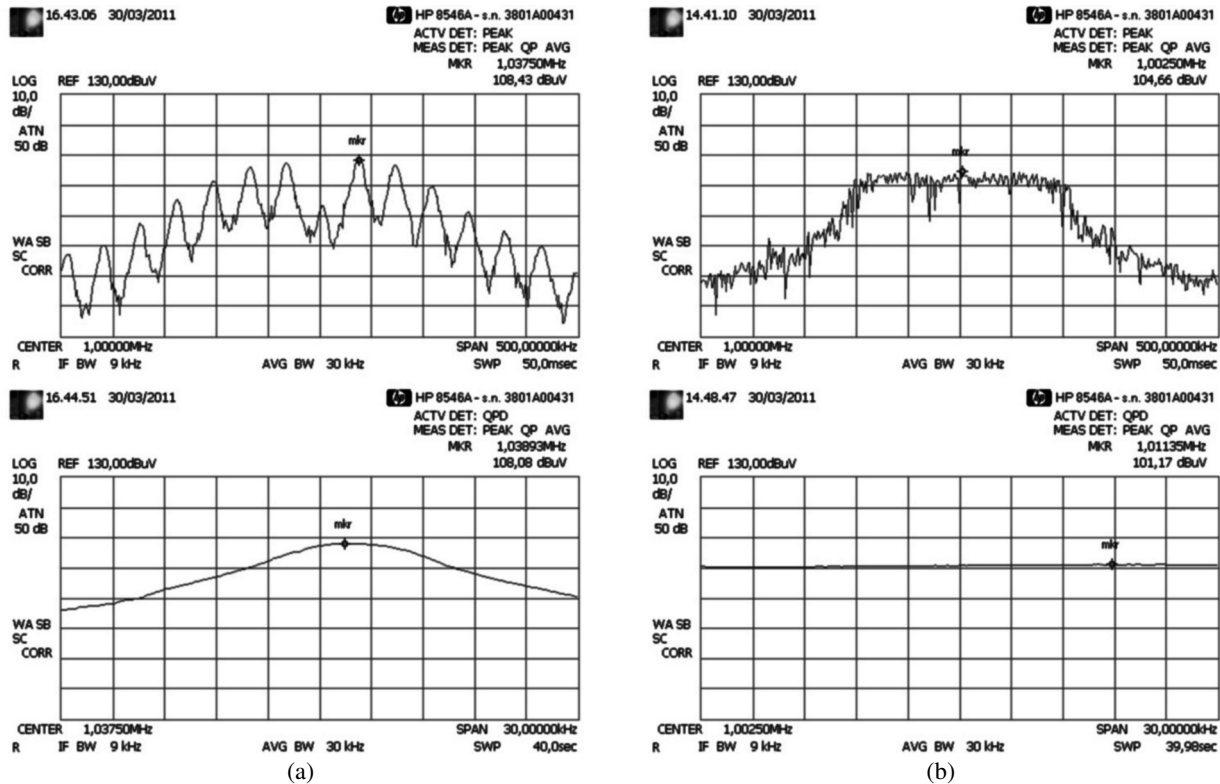


Figure 10. Comparison between the power spectra of first harmonic of the triangular-modulated clock (a) and of the chaotic-modulated clock (b), using both the peak detector (top) and the quasi-peak detector (bottom).